

Infrared Spectrum of the CH₃–PtH Complex in Solid Argon Prepared in the Oxidative C–H Insertion of Methane by Laser-Ablated Pt Atoms

Han-Gook Cho and Lester Andrews*

Department of Chemistry, University of Incheon, 177 Dohwa-dong, Nam-ku, Incheon, 402-749, South Korea, and Department of Chemistry, University of Virginia, P.O. Box 400319, Charlottesville, Virginia 22904-4319

Received: October 6, 2008; Revised Manuscript Received: October 30, 2008

Reactions of laser-ablated Pt atoms with CH₄ during condensation in excess argon form CH₃–PtH through oxidative C–H insertion show and that the late transition-metal atom Pt is an effective methane activation reagent, in agreement with gas phase investigations. Six observed infrared absorptions correlate with the six strongest calculated harmonic frequencies. The computed C–Pt bond length is slightly shorter than those of Pt complexes with large ligands. In addition, the strongest absorption of the CH₂=PtH₂ methylidene is detected.

The activation of C–H bonds is a key step in numerous synthetic reactions and catalytic processes.¹ Early investigations have shown that neutral metal atoms are often reactive under electronic excitation with small alkanes.² The C–H bond insertion of CH₄ by metal cations and particularly the Pt⁺ ion has been studied by ion beam and FT-ICR experiments.³ Recent studies reveal that many transition metals including lanthanides and actinides are good C–H insertion agents in reactions with small alkanes and often form high-oxidation-state complexes with a carbon–metal multiple bond following H migration.⁴ The higher oxidation-state complexes are more favored in general going down in a group and right among early transition metals. Although group 3–8 metals form the insertion and methylidene products, Re and Os produce carbyne complexes exclusively.^{4–6} However, small transition-metal complexes are expected to be less favored on going further right in the periodic table as more d-orbitals become filled.

Recently Zhou et al. have reported formation of CH₃–RhH in Rh atom reactions with CH₄ during annealing in a cold Ar matrix.⁷ These workers failed to observe a reaction product on codeposition of Pt with methane in excess argon under the conditions of their experiment and on subsequent broadband irradiation or annealing. Theoretical studies for the C–H bond insertion process by transition metals have predicted reactivity with a low (2.1 kcal/mol) activation barrier for the platinum atom insertion reaction with methane.⁸ Furthermore, Carroll et al. have measured the reaction rate of Pt with small alkanes by monitoring the laser induced fluorescence from the metal atom and found ground-state Pt to be unique among neutral transition metal atoms in its reaction with methane at 300 K.⁹ In addition, the reaction efficiency of Pt increases with the number of carbons in the alkane chain. Their calculations indicate that CH₃–PtH is a stable product and suggest that a large potential energy barrier prohibits H₂ elimination.

Matrix isolation studies have shown that only Pt among group 10 metals forms C–H insertion complexes in reactions of laser-ablated Pt atoms with C₂H₂ and C₂H₄.¹⁰ More recently, small

Pt methylidene complexes with substantial double bond character from d_π–p_π bonding have been produced in reactions of Pt with tetrahalomethanes.¹¹ Here, we report infrared spectra of isotopic products from reactions of laser-ablated Pt atoms with methane. The products are identified by isotopic substitution and vibrational frequency calculations.

Laser ablated Pt atoms were reacted with CH₄ (Matheson, UHP grade), ¹³CH₄, CD₄, and CH₂D₂ (Cambridge Isotopic Laboratories) in excess argon during condensation at 10 K using a closed-cycle refrigerator (Air Products Displex). These methods have been described in detail elsewhere.¹² After reaction, infrared spectra were recorded at a resolution of 0.5 cm⁻¹ using a Nicolet 550 spectrometer with a HgCdTe range B detector. Samples were irradiated for 20 min periods by a mercury arc street lamp through optical glass filters, annealed, and more spectra were recorded.

Complementary density functional theory (DFT) calculations were carried out using the Gaussian 03 package,¹³ the B3LYP density functional, 6-311++G(3df,3pd) basis sets for C, H, and SDD pseudopotential and basis for Pt to provide a consistent set of vibrational frequencies for the reaction products. BPW91 functional and more rigorous CCSD calculations were also done to complement the B3LYP results. The vibrational frequencies were calculated analytically except for the CCSD method. Zero-point energies are included in the calculation of binding energies.

Figure 1 shows the regions in the infrared spectra of product absorptions from reactions of Pt with CH₄, CD₄, ¹³CH₄, and CH₂D₂. The major product absorptions are marked with “i” (i for insertion); their intensities remain the same upon visible (λ > 420 nm), increase 10% on UV (240 < λ < 380 nm) irradiation and later decrease on sample annealing. The product frequencies are compared with calculated values in Table 1. The diagnostic i absorption at 2315.9 cm⁻¹ shows no ¹³C shift and a D shift to 1661.7 cm⁻¹ (H/D frequency ratio 1.394). These new bands are between PtH (2280.4 cm⁻¹) and PtH₂ frequencies of 2365.7 and 2348.9 cm⁻¹ or PtD (1634.0 cm⁻¹) and PtD₂ frequencies of 1697.7 and 1683.3 cm⁻¹, which were observed in the reaction with hydrogen or deuterium.¹⁴ This single observed Pt–H stretching absorption provides strong evidence

* Author to whom correspondence should be addressed. E-mail: lsa@virginia.edu.

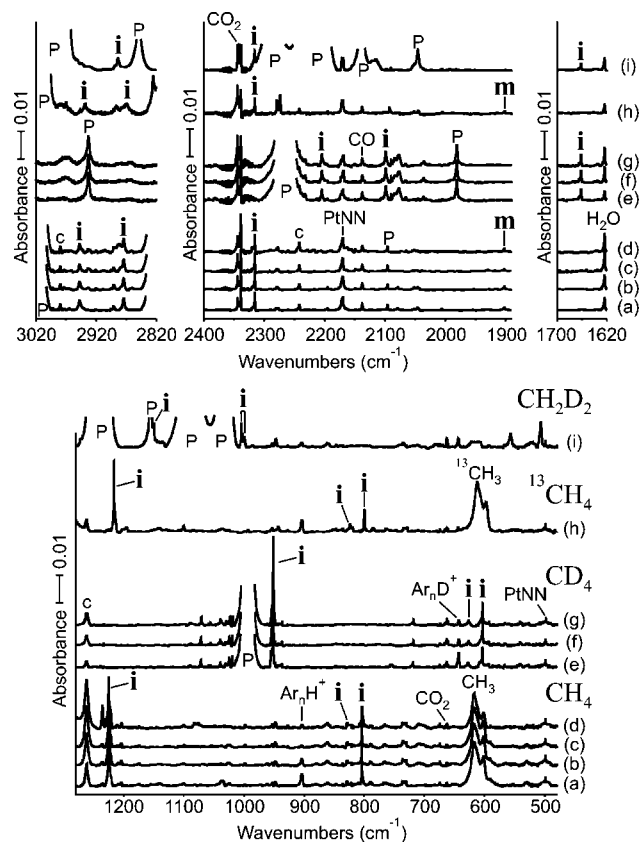


Figure 1. Infrared spectra in the product absorption regions from laser-ablated Pt atom reactions with CH_4 isotopomers in excess argon at 10 K. (a) Pt + 1.0% CH_4 in Ar codeposited for 1 h. (b) After photolysis ($\lambda > 420$ nm). (c) After photolysis ($240 < \lambda < 380$ nm). (d) After annealing to 28 K. (e) Pt + 1.0% CD_4 in Ar. (f) After photolysis ($240 < \lambda < 380$ nm). (g) After photolysis ($\lambda > 220$ nm). (h) Pt + 1.0% $^{13}\text{CH}_4$ in Ar. (i) Pt + 2.0% CH_2D_2 in Ar. **i** and **m** denote product absorptions. **P** indicates precursor absorptions and **c** denotes product absorptions common to methane and other metals. CO_2 , PtNN, CO, Ar_nH^+ and CH_3 absorptions are also designated.

for formation of the C–H insertion complex, $\text{CH}_3\text{-PtH}$. At the B3LYP level without accounting for spin orbit effects, the insertion complex is the most stable plausible product: $\text{CH}_3\text{-PtH}$ and $\text{CH}_2=\text{PtH}_2$ in their singlet ground states are 35 and 4 kcal/mol more stable than the reactants ($\text{CH}_4 + \text{Pt}(^3\text{D})$). Our energy for $\text{CH}_3\text{-PtH}$ is in good agreement with those from PCI-80 calculations corrected for spin–orbit effects (27 or 32 kcal/mol).^{8,9}

The strong A' CH_3 deformation absorption of the insertion complex is observed at 1225.9 cm^{-1} , and its D and ^{13}C counterparts at 952.1 and 1216.3 cm^{-1} (H/D and 12/13 ratios of 1.288 and 1.008). The A' and A'' CH_3 rocking bands at 828.4 and 804.1 cm^{-1} have their D counterparts at 627.5 and 604.3 cm^{-1} (H/D ratios of 1.320 and 1.331) and their ^{13}C counterparts at 823.9 and 800.0 cm^{-1} (12/13 ratios of both 1.005). In the high-frequency region, two CH_3 stretching frequencies are also observed at 2947.6 and 2874.6 cm^{-1} , their D counterparts at 2205.0 and 2099.0 cm^{-1} (H/D ratios of 1.337 and 1.370), and their ^{13}C counterparts at 2939.8 and 2869.6 cm^{-1} . Table 1 shows that the six new product absorptions are in fact the strongest bands predicted for $\text{CH}_3\text{-PtH}$ in its ground $^1A'$ state and that the observed frequencies correlate nicely with the calculated values (for example, the B3LYP harmonic values range from 4.6 to 1.0% higher than the observed bands),¹⁵ which substantiate formation of the insertion product, $\text{CH}_3\text{-PtH}$.

Additional support comes from the Pt reaction with CH_2D_2 (Figure 1). First notice that the diagnostic 2316.1 and 1661.6 cm^{-1} product absorptions are essentially the same wavenumbers as with CH_4 and CD_4 and in 2/1 relative intensity. Our calculations (Table 1) find the Pt–H infrared absorption to be double the intensity of the Pt–D absorption, which shows that equal yields of $\text{CH}_2\text{D-PtD}$ and $\text{CHD}_2\text{-PtH}$ are produced, and there appears to be no kinetic isotope effect on C–H(D) activation with laser ablated Pt atoms. Both C_s and C_1 structures are possible for the mixed isotopic products, and our calculations find the two isomer Pt–H modes within 0.24 cm^{-1} and the two isomer Pt–D modes within 0.05 cm^{-1} , which we cannot resolve. The two CH_2D , CHD_2 deformation modes observed at 1151.2 and 1004.6 cm^{-1} fall within the pure isotopic values, and are consistent with either structure. The observed bands are listed with the C_s structures in Table S1, Supporting Information, although frequencies computed for the C_1 structure are also compatible.

Weak product absorptions are also observed at 1901.6 cm^{-1} in the CH_4 and $^{13}\text{CH}_4$ spectra (labeled **m** for methylidene, Figure 1a–d,h) and at 1365.8 cm^{-1} in the CD_4 spectra (not shown) (H/D frequency ratio 1.392). They are compared with the B3LYP calculated harmonic frequencies of 1917.8 and 1364.5 cm^{-1} for the very strong, PtH_2 antisymmetric stretching mode of $\text{CH}_2=\text{PtH}_2$ and the deuterated isotopomer (Table S2, Supporting Information). Though more evidence is needed to identify conclusively the higher oxidation-state complex, these bands are appropriate for its strongest infrared absorption. The

TABLE 1: Observed and Calculated Fundamental Frequencies of $\text{CH}_3\text{-PtH}$ Isotopomers in the $^1A'$ Ground State^a

approximate description	$\text{CH}_3\text{-PtH}$				$\text{CD}_3\text{-PtD}$				$^{13}\text{CH}_3\text{-PtH}$						
	obs	B3LYP	int	BPW91	CCSD	obs	B3LYP	int	BPW91	CCSD	obs	B3LYP	int	BPW91	CCSD
A'' CH_3 str		3120.9	2	3057.6	3147.4	2314.6	0	2267.3	2333.0		3109.2	2	3046.2	3135.8	
A' CH_3 str	2947.6	3082.4	12	3020.1	3108.9	2277.4	5	2232.1	2296.6	2938.8	3072.7	12	3010.4	3099.1	
A' CH_3 str	2874.6	2983.4	15	2920.0	3007.1	2136.9	9	2090.2	2154.8	2969.6	2979.7	14	2916.7	3003.5	
A' Pt–H str	2315.9	2412.4	14	2416.8	2596.5	1661.7	1710.9	7	1714.1	1841.5	2315.9	2412.4	14	2416.8	2596.5
A' CH_3 scis		1456.7	0	1407.7	1483.3	1059.8	0	1024.2	1077.4		1453.2	0	1404.3	1480.0	
A'' CH_3 deform		1429.2	2	1378.9	1452.0	1039.6	2	1003.1	1054.8		1425.8	2	1375.6	1448.7	
A' CH_3 deform	1225.2	1256.1	38	1214.3	1301.3	952.1	23	939.7	1013.3	1216.3	1248.2	38	1206.7	1292.4	
A' CH_3 rock	828.4	845.8	14	829.8	891.9	627.5	634.6	8	622.9	671.3	823.9	841.0	14	825.1	886.6
A'' CH_3 rock	804.1	812.3	18	792.1	836.7	604.3	602.4	10	587.6	622.4	800.0	808.6	18	788.4	832.6
A' C–Pt str		604.0	4	603.4	644.1		541.5	0	542.4	571.8		588.5	5	587.0	628.3
A' HPtC bend		494.6	19	477.1	534.4		357.0	11	343.1	386.3		492.3	18	475.6	531.5
A'' CH_3 distort		155.7	8	158.7	189.1		110.3	4	112.5	134.0		155.7	8	158.7	189.1

^aFrequencies and intensities are in cm^{-1} and km/mol . Observed in an argon matrix. Frequencies and intensities are computed with 6-311+G(3df, 3pd), and the SDD core potential and basis set are used for Pt. Intensities are calculated with B3LYP. $\text{CH}_3\text{-PtH}$ has a C_s structure with two equal C–H bonds, and symmetry notations are based on the C_s structure.

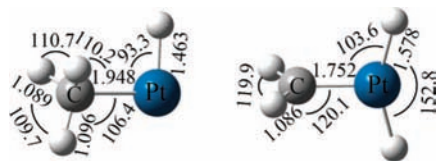


Figure 2. Structures of $\text{CH}_3\text{-PtH}$ and $\text{CH}_2\text{=PtH}_2$ calculated using CCSD and 6-311++G(3df,3pd)/SDD. $\text{CH}_3\text{-PtH}$ has a C_s structure and $\text{CH}_2\text{=PtH}_2$ a C_{2v} structure. Bond lengths and angles are in Å and deg.

Pt–H stretching band absorbance ratio for the **i** and **m** products, 8/1, normalized by the computed infrared intensities, suggests that about 1% of the $\text{CH}_3\text{-PtH}$ undergoes $\alpha\text{-H}$ transfer to $\text{CH}_2\text{=PtH}_2$ during relaxation in the matrix. An analogous mechanism has been invoked in the formation of $\text{CCl}_2\text{=PtCl}_2$.¹¹

Pt (excited by laser ablation) +



Computed CCSD structures of the Pt reaction products are illustrated in Figure 2. $\text{CH}_3\text{-PtH}$ has a C_s structure at all levels of theory used in this study, and the C–Pt bond length 1.948 Å is shorter than in typical Pt complexes (~ 2.0 Å).¹⁶ The methyldene $\text{CH}_2\text{=PtH}_2$ has the C_{2v} structure with perpendicular CH_2 and PtH_2 planes and 1.752 Å C=Pt bond length similar to $\text{CCl}_2\text{=PtCl}_2$.¹¹

We must explain the lack of an observable reaction product in the apparently similar experiments of Zhou et al.⁷ There are, however, critical differences in how these experiments are done. First, the absorptions of $\text{CH}_3\text{-PtH}$ are not intense so a high product yield is needed for detection. Laser energy and laser focus are experimental variables, and our group typically uses higher laser energy and produces a higher product yield, and this is likely the case with the refractory metal Pt. Second, we employ the ten times more sensitive liquid nitrogen cooled Hg–Cd–Te range B detector than the deuteriated triglycine sulfate detector used in Fudan. Third, our condensing surface is stated to be colder (by 2 K and this effect will depend heavily on maximum thermal contact between the cold surface and the sample substrate), and thus we will trap reaction products more efficiently on sample codeposition.

The formation of $\text{CH}_3\text{-PtH}$ on codeposition of laser-ablated Pt atoms with methane in excess argon clearly shows that the neutral Pt atom is an efficient C–H insertion agent, and because

CH_4 is the least reactive for C–H insertion,⁹ similar reactions are expected to occur for other hydrocarbons. In this regard, matrix isolation experiments with ethane have produced the $\text{CH}_3\text{CH}_2\text{-PtH}$ complex.

Acknowledgment. We gratefully acknowledge financial support from NSF Grant CHE 03-52487 to L.A., and the use of the computing system of the KISTI Supercomputing Center (KSC-2008-S02-0001) is also greatly appreciated.

Supporting Information Available: Tables S1 and S2 comparing observed and calculated frequencies. This material is available free of charge via the Internet at <http://pubs.acs.org>.

References and Notes

- (1) (a) Davies, H. M.; Beckwith, R. E. *J. Chem. Rev.* **2003**, *103*, 2861. (b) Campos, K. R. *Chem. Soc. Rev.* **2007**, *36*, 1069. (c) Díaz-Requejo, M. M.; Pérez, P. *Chem. Rev.* **2008**, *108*, 3379.
- (2) (a) Davis, S. C.; Klabunde, K. J. *J. Am. Chem. Soc.* **1978**, *100*, 5973. (b) Billups, W. E.; Konarski, M. M.; Hauge, R. H.; Margrave, J. L. *J. Am. Chem. Soc.* **1980**, *102*, 7393.
- (3) (a) Zhang, X.-G.; Liyanage, R.; Armentrout, P. B. *J. Am. Chem. Soc.* **2001**, *123*, 5563. (b) Heinemann, C.; Wesendrup, R.; Schwarz, H. *Chem. Phys. Lett.* **1995**, *239*, 75.
- (4) Andrews, L.; Cho, H.-G. *Organometallics* **2006**, *25*, 4040, and references therein.
- (5) Cho, H.-G.; Andrews, L. *Inorg. Chem.* **2008**, *47*, 1653 (Re + CH_4).
- (6) Cho, H.-G.; Andrews, L. *Organometallics* **2008**, *27*, 1786 (Os + CH_4).
- (7) Wang, G; Chen, M.; Zhou, M. *Chem. Phys. Lett.* **2005**, *412*, 46 (Rh + CH_4).
- (8) Wittborn, A. M. C.; Costas, M.; Blomberg, M. R. A.; Siegbahn, P. E. M. *J. Chem. Phys.* **1997**, *107*, 4318, and references therein.
- (9) Carroll, J. J.; Weisshaar, J. C.; Siegbahn, P. E. M.; Wittborn, C. A. M.; Blomberg, M. R. A. *J. Phys. Chem.* **1995**, *99*, 14388.
- (10) (a) Wang, X.; Andrews, L. *J. Phys. Chem. A* **2004**, *108*, 4838. (b) Cho, H.-G.; Andrews, L. *J. Phys. Chem. A* **2004**, *108*, 6272.
- (11) Cho, H.-G.; Andrews, L. *J. Am. Chem. Soc.* **2008**, in press (Pt + CX_4).
- (12) (a) Andrews, L.; Citra, A. *Chem. Rev.* **2002**, *102*, 885, and references therein. (b) Andrews, L. *Chem. Soc. Rev.* **2004**, *33*, 123, and references therein.
- (13) Frisch, M. J.; et al. *Gaussian 03*, revision C.02; Gaussian, Inc.: Pittsburgh, PA, 2003.
- (14) Andrews, L.; Wang, X.; Manceron, L. *J. Chem. Phys.* **2001**, *114*, 1559.
- (15) (a) Scott, A. P.; Radom, L. *J. Phys. Chem.* **1996**, *100*, 16502. (b) Andersson, M. P.; Uvdal, P. L. *J. Phys. Chem. A* **2005**, *109*, 3937.
- (16) (a) Newman, C. P.; Deeth, R. J.; Clarkson, G. J.; Rourke, J. P. *Organometallics* **2007**, *26*, 6225. (b) Fang, M.; Jones, N. D.; Ferguson, M. J.; McDonald, R.; Cavell, R. G. *Angew. Chem., Int. Ed.* **2005**, *44*, 2005. (c) Hanks, T. W.; Ekeland, R. A.; Emerson, K.; Larsen, R. D.; Jennings, P. W. *Organometallics* **1987**, *6*, 28.

JP8088325